

Article

Recovery of Alkaline Earth Metals from Desalination Brine for Carbon Capture and Sodium Removal

Cheng-Han Lee ¹, Pin-Han Chen ² and Wei-Sheng Chen ^{1,*}

¹ Department of Resources Engineering, National Cheng Kung University, No. 1, Daxue Rd., East Dist., Tainan City 70101, Taiwan; n48091013@gs.ncku.edu.tw

² Tainan Hydraulics Laboratory, National Cheng Kung University, No. 500, Sec. 3, Anming Rd., Annan Dist., Tainan City 709015, Taiwan; hannah83530@thl.ncku.edu.tw

* Correspondence: kenchen@mail.ncku.edu.tw; Tel.: +886-6-2757575 (ext. 62828)

Abstract: Because carbon dioxide adsorbs the radiation from the Sun and the Earth's surface, global warming has become a severe problem in this century. Global warming causes many environmental problems such as heatwave, desertification, and erratic rainfall. Above all, erratic rainfall makes people have insufficient freshwater. To solve this problem, desalination technology has been developed in many countries. Although desalination technology can provide freshwater, it produces brine as well (producing 1 L of freshwater would result in 1 L of brine). The brine will decrease the dissolved oxygen in the sea and affect the organism's habitat. In this study, magnesium and calcium from desalination brine were recovered in the form of magnesium hydroxide and calcium hydroxide by adjusting the pH value for carbon capture and sodium removal. Magnesium hydroxide would turn into magnesium carbonate through contacting CO₂ in saturated amine carriers. Calcium hydroxide was added to the brine and reacted with CO₂ (modified Solvay process). Sodium in brine would then be precipitated in the form of sodium bicarbonate. After removing sodium, brine can be released back into the ocean, or other valuable metals can be extracted from brine without the side effect of sodium. The results revealed that 288 K of 3-Amino-1-propanol could capture 15 L (26.9 g) of CO₂ and that 25 g/L of Ca(OH)₂ at 288 K was the optimal parameter to remove 7000 ppm sodium and adsorb 16 L (28.7 g) of CO₂ in the modified Solvay process. In a nutshell, this research aims to simultaneously treat the issue of CO₂ emission and desalination brine by combining the amines carrier method and the modified Solvay process.



Citation: Lee, C.-H.; Chen, P.-H.; Chen, W.-S. Recovery of Alkaline Earth Metals from Desalination Brine for Carbon Capture and Sodium Removal. *Water* **2021**, *13*, 3463. <https://doi.org/10.3390/w13233463>

Academic Editor: Thomas M. Missimer

Received: 5 November 2021

Accepted: 3 December 2021

Published: 6 December 2021

Keywords: recovery; desalination brine; amine carrier; modified Solvay process; carbon capture; sodium removal; magnesium; calcium

1. Introduction

Carbon dioxide (CO₂) is the principal reason for the greenhouse effect, global warming, and climate change [1–5]. The global average temperature increases when the concentration of CO₂ rises and causes many extreme climate events such as heatwave, desertification, and erratic rainfall. Among them, erratic rainfall makes people have insufficient freshwater. According to a survey of the United Nations (UN), more than 1 billion people in the world will live in areas with scarce water resources by 2025 [6]. To solve the problem, desalination technology has been developed since the 1950s [7]. However, when desalination technology is ordinary, the by-product of desalination, brine, also brings about considerable harm to the environment. For example, the brine will decrease the dissolved oxygen in the sea and affect the organism's habitat. Besides, producing 1 L of freshwater will generate 1 L of brine, demonstrating that the amount of brine from desalination plants is equal to freshwater. To solve these problems simultaneously, brine is used for CO₂ capture to enhance its value (Avoiding releasing it directly into the ocean).

Carbon capture and utilization (CCU) can be mainly divided into organic CCU and inorganic CCU [8–10]. In organic CCU, the processes require a high temperature, pressure,

Publisher's Note: MDPI stays neutral with regard to jurisdictional claims in published maps and institutional affiliations.



Copyright: © 2021 by the authors. Licensee MDPI, Basel, Switzerland. This article is an open access article distributed under the terms and conditions of the Creative Commons Attribution (CC BY) license (<https://creativecommons.org/licenses/by/4.0/>).

and catalysts to produce valuable organic compounds; therefore, this requires much money in order to reach the goal of industrialization and commercialization. In inorganic CCU, the energy consumption is much lower than organic CCU due to the lower temperature and pressure during the processes. It can also use many materials such as amine [11], ammonia [12–15], alkaline materials [16], solid wastes [17–22], fly ash [23–26], cement [27], wastewater [28,29], and brine to capture CO₂ [30–32]. In the inorganic CCU method, magnesium and calcium are the chief elements for capturing CO₂ due to their high reaction with CO₂ and their obtainability. CO₂ can be absorbed and turned into magnesium carbonate and calcium carbonate, which will be utilized in coating materials, food additives, and medicines. Due to the importance of magnesium and calcium, some research has suggested separating them from desalination brine and using them to capture CO₂ through the amine carrier method and the modified Solvay process [33–36]. The outputs of previous research are shown in Table 1.

Table 1. The outputs of previous research.

Author	Method	Process and Results
D. Kang et al. [33]	Amine carrier method	0.79, 0.34 and 0.19 mol of CO ₂ was captured by 5, 10 and 30 wt% of aqueous MEA solutions, separately. When pretreated brine solutions were added to each saturated MEA solution, CO ₂ was turned into CaCO ₃ . Through analyses, it was proven that the CaCO ₃ was in the form of calcite.
Y. Yoo et al. [34]	Amine carrier method	CO ₂ was captured by different amines and carried into the separated Ca(OH) ₂ to generate CaCO ₃ . XRD, SEM, FT-IR and TG/DTG analyses were used to investigate the crystal shape, polymorph, and purity of the product. The results illustrated that crystallization inhibition was possible, depending on the structural properties of amine carriers, leading to a successful CaCO ₃ polymorph control.
M.H. El-Naas et al. [36]	Modified Solvay process	The authors replaced ammonia with calcium oxide to conduct a CO ₂ capture. In this modified Solvay process, each mole of Ca(OH) ₂ could capture two moles of CO ₂ . Moreover, calcium hydroxide could be directly obtained from brine by adjusting the pH value. Under the optimal conditions, a CO ₂ capture of 86% and 99% and sodium removal of 29% and 35% were achieved for the traditional Solvay and the modified process, respectively.

The Amine carrier method uses amine to adsorb CO₂ first, and alkaline earth metals can react with the saturated amines to form bicarbonate solutions or carbonate compounds. Since the magnesium and calcium in the brine are abundant, brine can be applied to this method. The pH value of brine can be adjusted to a strong base to precipitate magnesium hydroxide and calcium hydroxide for a reaction with amines. The merits of this process are that it does not need too much energy consumption and can produce valuable products. The other method, the modified Solvay process, is the improvement of the Solvay process. The Solvay process is the primary industrial process for producing sodium carbonate, and the ingredients for this are salt and limestone. The Solvay process is related to desalination brine and CO₂ capture because salt can be collected from brine, and it can react with CO₂, H₂O, and NH₃ to generate sodium bicarbonate and ammonium chloride (Equation (1)). Although this process is inexpensive and convenient, ammonia volatilizes easily and is harmful to humans [37]. In this case, calcium hydroxide from desalination brine replaces ammonia to decrease the danger in the process (Equation (2)) [36]. The other advantage of calcium hydroxide is that it can increase the pH value of the system so that the CO₂ can be adsorbed more than the ammonia system.



This research used brine for carbon capture and sodium removal through the amine carrier method and the modified Solvay process. Brine would be adjusted to pH 9–14 to precipitate magnesium hydroxide and calcium hydroxide. Magnesium hydroxide would react with saturated amine carriers to produce magnesium bicarbonate solutions. Magnesium carbonate would then be obtained by heating the amine carriers, and the amine carriers could be reused after the magnesium carbonate precipitated. The amine carriers applied in this study were 3-Amino-1-propanol, ethylamine, and diethylenetriamine. The CO₂ saturated adsorption capacity of three amine carriers and the CO₂ saturated adsorption capacity of an optimal amine carrier under different temperatures were surveyed in this study. After adsorbing CO₂ and collecting magnesium carbonate, calcium hydroxide would be used for the modified Solvay process. As shown in Equation (2), sodium bicarbonate would be precipitated, and the precipitation rate concerned the concentration of calcium hydroxide and the contacting temperature. To realize the relationship between them, different concentrations of calcium hydroxide and temperatures of brine would be investigated. After capturing CO₂ and removing sodium, the brine could be released back into the ocean, or other valuable elements such as lithium, rubidium, and cesium could be extracted without the side effect of sodium. In a nutshell, this study combines the amine carrier method and the modified Solvay process. The parameters such as the magnesium hydroxide and calcium hydroxide precipitation rate, saturated CO₂ adsorption capacity of amine carriers, and sodium removal rate were discussed. The detection of magnesium carbonate through methods such as X-ray diffraction (XRD), scanning electron microscopy (SEM), and whiteness analyses were explored as well, in order to confirm its practicality. This research aims to increase the added value of brine and decrease CO₂ emissions simultaneously.

2. Experimental Section

2.1. Reagents and Chemicals

Desalination brine was generated from the desalination plant in Taiwan, and its main elements and concentrations are shown in Table 2. Lithium hydroxide ($\geq 98\%$) was obtained from Sigma-Aldrich (St. Louis, MO, USA) to regulate the pH value of brine, and magnesium hydroxide and calcium hydroxide were precipitated. 3-Amino-1-propanol ($\geq 99\%$), ethylamine (97%), and diethylenetriamine (99%) were acquired from Sigma-Aldrich (St. Louis, MO, USA) to capture CO₂ in the amine carrier method, and their chemical structures are demonstrated in Figure 1a–c. According to Figure 1, one can see that three amines are alkanolamine, alkylamine, and multi-amine, respectively. CO₂ gas was procured from Yun Shan Gas Co. (Tainan, Taiwan) and combined with N₂ in the ratio of 15:85. In the analysis procedure, ICP standard solution was purchased from High-Purity Standards, Inc. (North Charleston, SC, USA). The nitric acid ($\geq 65\%$) was from Sigma-Aldrich (St. Louis, MO, USA) and diluted to 1% to be the thinner for the ICP analysis. Additionally, all chemicals were analytical grade and applied without further purification. The resistivity of deionized water used in the whole process was 18.0 MΩ.cm to avoid impurities affecting the results.

Table 2. The main elements and the concentrations of desalination brine.

Elements	Na	Mg	K	Ca	Rb	Li	B
Concentration (mg/L)	17,420	2112	782.6	722.2	36.4	19.5	18.9

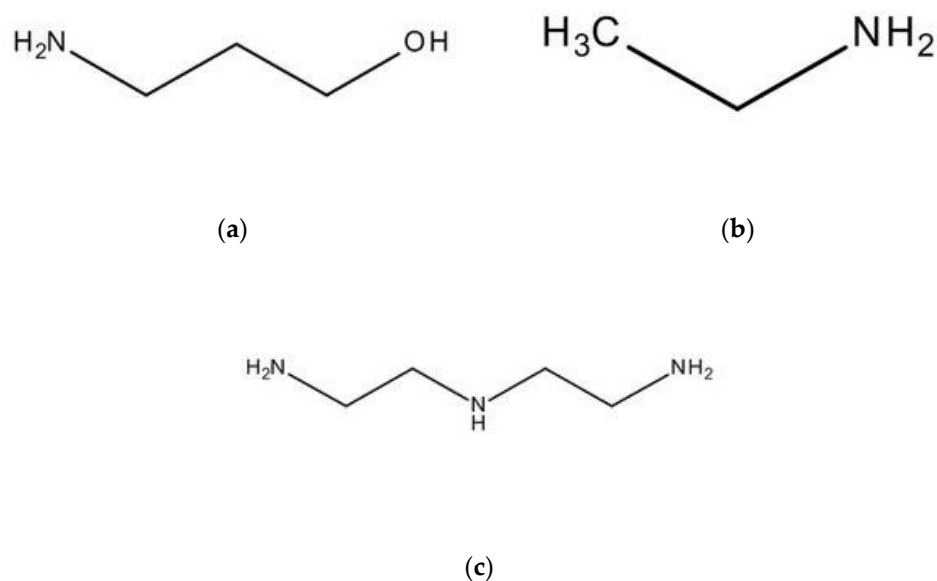


Figure 1. The chemical structure of (a) 3-Amino-1-propanol, (b) ethylamine, and (c) diethylenetriamine.

2.2. Apparatus

The CO₂ capture was operated through a CO₂ adsorption system in the amine carrier method and modified Solvay process. The whole system is displayed in Figure 2. In this study, 2.5 M of amine carriers (0.5 mol of amine carrier was dissolved in 200 mL deionized water) or brine mixed with Ca(OH)₂ were placed into the reactor. 15% of CO₂ gas with 85% of N₂ gas were controlled by a mass flow controller (MFC, Taiwan Puritic Corp., Hsinchu, Taiwan) before being pumped into the reactor, and MFC was able to maintain the reactor's pressure at 1 bar. After being pumped into the reactor, a temperature controller (XMtd-204; BaltaLab, Vidzemes priekšpilsēta, Rīga, Latvia) maintained the temperature in the process. When the reaction finished, there were a gas analyzer and computer to analyze the CO₂ concentration of effluent gas and make us calculate the CO₂ adsorption capacity in the form of L CO₂/mol amine and L CO₂/L brine (Equations (3) and (4)). The adsorption process was terminated when the analyzer detected that the CO₂ concentration of effluent gas was 15%. This reveals that the amine carriers and brine could no longer adsorb CO₂. Besides, the gas was transmitted by the PTFE pipes during this whole experiment to secure no gas emissions.

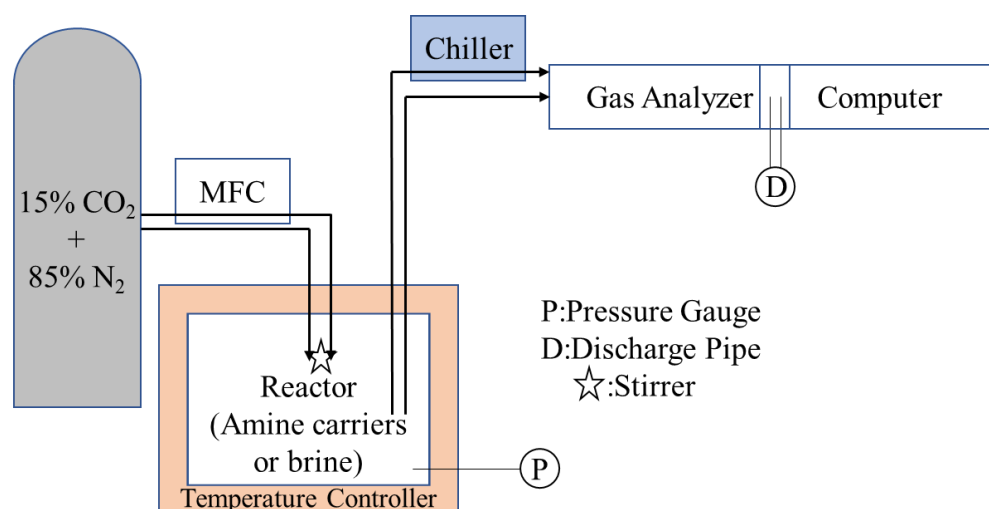


Figure 2. The CO₂ adsorption system in this study.

After magnesium hydroxide reacted with saturated amine carriers, magnesium carbonate was analyzed by X-ray diffraction (XRD, DX-2700, Dandong City, Liaoning Province, China) and scanning electron microscopy (SEM, S-3000N, Hitachi, Tokyo, Japan). The magnesium, calcium, and sodium precipitation efficiencies were detected by inductively coupled plasma optical emission spectrometry (ICP-OES, Varian, Vista-MPX, PerkinElmer, Waltham, MA, USA). On the other hand, the whiteness of magnesium carbonate was detected by a whiteness meter (Pora Volo-W, JIN-BOMB Enterprise Co., Ltd., Kaohsiung, Taiwan) to confirm its applied value.

$$\text{CO}_2 \text{ adsorption capacity} \left(\frac{\text{L CO}_2}{\text{mol Amine}} \right) = \frac{\Sigma \text{L CO}_2 \text{ capture}}{\text{mol Amine}} \quad (3)$$

$$\text{CO}_2 \text{ adsorption capacity} \left(\frac{\text{L CO}_2}{\text{L Brine}} \right) = \frac{\Sigma \text{L CO}_2 \text{ capture}}{\text{L Brine}} \quad (4)$$

3. Results and Discussion

3.1. The Recovery Rate of Magnesium Hydroxide and Calcium Hydroxide

At the beginning of the experiment, lithium hydroxide was added into the brine to precipitate magnesium hydroxide and calcium hydroxide under the condition of 298 K and 10 min. The original pH value of brine was 8.14, so the parameters were set up from pH 9 to pH 14. The precipitation efficiency was calculated as Equation (5), and the precipitation rates of magnesium and calcium at different pH values are shown in Figure 3. As Figure 3 reveals, magnesium could be precipitated as the pH value of the solution increased from 9 to 12, and the precipitation rate of magnesium hydroxide was 99.94% (2112 mg/L to 1.175 mg/L). On the other hand, calcium hydroxide was mainly precipitated at pH 14, and the precipitation rate was 97.2% (722.16 mg/L to 19.57 mg/L). The precipitated magnesium hydroxide and calcium hydroxide were then applied to the amine carrier method and modified Solvay process, respectively.

$$P (\%) = \frac{[M]_0 - [M]}{[M]_0} \cdot 100 \quad (5)$$

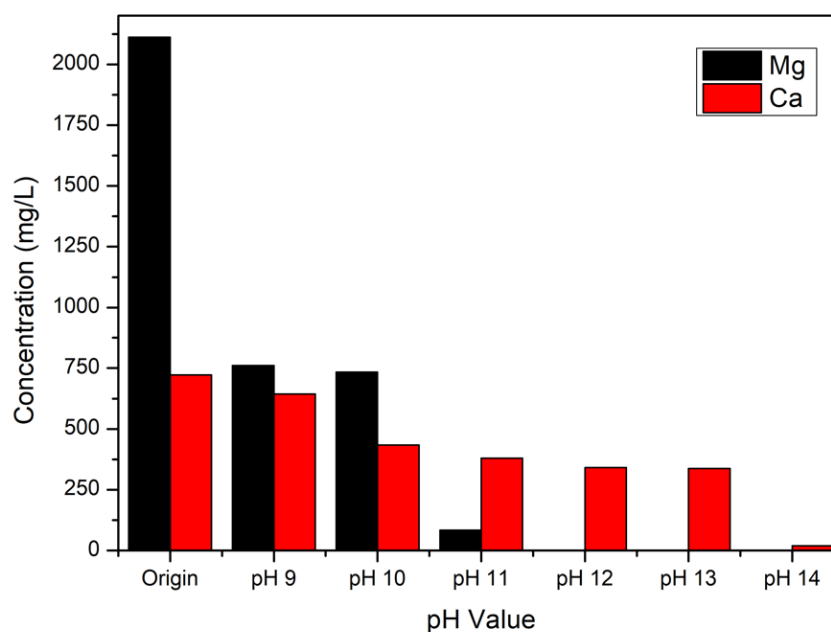


Figure 3. Precipitation efficiencies of magnesium hydroxide and calcium hydroxide.

P is the precipitation efficiency, $[M]_0$ is the metal (Mg and Ca) concentration of brine, and $[M]$ is the metal concentration (Mg and Ca) of brine after the precipitation process.

3.2. Amine Carrier Method- CO_2 Adsorption Capacities of Different Amine Carriers

Before magnesium hydroxide reacted with saturated amine carriers, the adsorption capacities of different amine carriers should be explored first. Figure 4a–c reveals the saturated CO_2 adsorption capacities of 3-Amino-1-propanol, ethylamine, and diethylenetriamine under the condition of 288 K. In Figure 4, the trends of the three amine carriers are similar. The CO_2 adsorption capacities rose when time increased. However, their saturated capacities and time were totally different. Their saturated CO_2 adsorption capacities were 15.1 L, 9 L, and 15.2 L per mol amines at about 150 min, 50 min, and 300 min, respectively. The CO_2 adsorption capacities were affected by the ethyl group, so the saturated capacities were highest when using diethylenetriamine in this experiment. However, the stability of diethylenetriamine was dependent on the number of amino groups [34]. Its viscosity might enlarge when CO_2 was dissolved. The enlarged viscosity made the reaction challenging to conduct, so the period of the experiment was most extended among the three amine carriers.

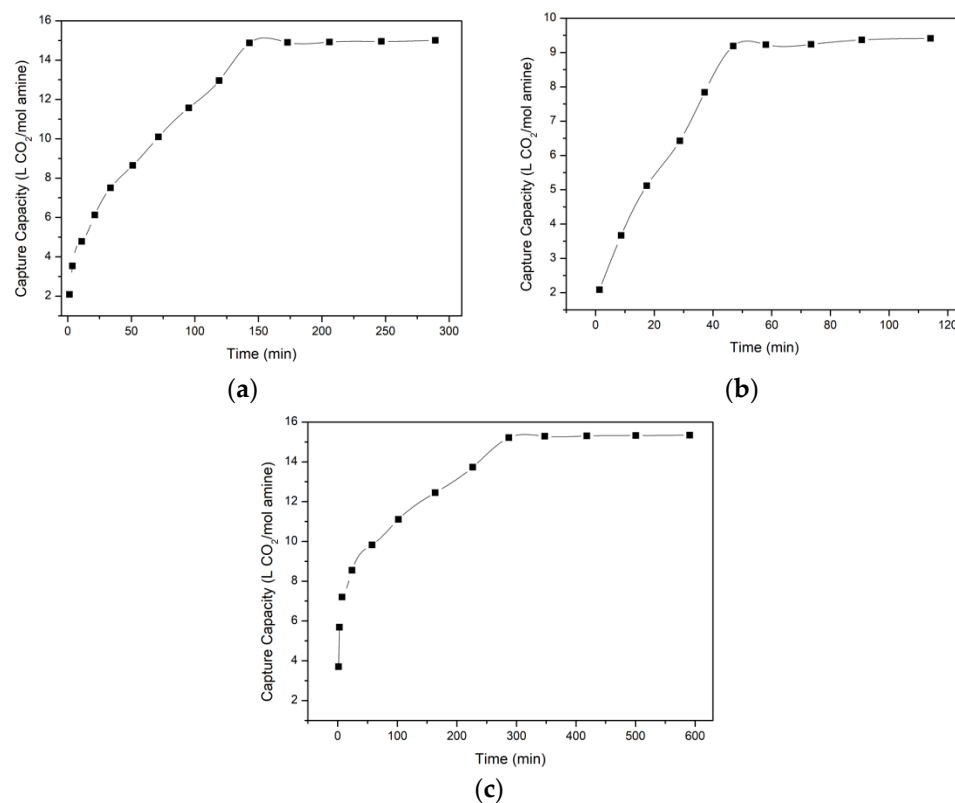


Figure 4. The saturated CO_2 adsorption capacities of (a) 3-Amino-1-propanol, (b) ethylamine, and (c) diethylenetriamine.

Although the reacting time of ethylamine was shorter and the adsorption capacity of diethylenetriamine was higher in this research, ethylamine and diethylenetriamine are more volatile than 3-Amino-1-propanol (Ethylamine and diethylenetriamine would produce fogs). Besides, it was also found that the temperature of diethylenetriamine during the adsorbing process would increase and enhance the temperature controller's energy consumption. For the sake of more carbon dioxide, safety, and a lower energy consumption, 3-Amino-1-propanol was chosen as the optimal amine carrier in this study.

3.3. Amine Carrier Method-CO₂ Adsorption Capacities of 3-Amino-1-Propanol at Different Temperatures

The temperatures of 3-Amino-1-propanol were set up from 288 K to 328 K in this part, and the concentration of 3-Amino-1-propanol was 2.5 M. Figure 5 illustrates that lower temperatures of 3-Amino-1-propanol could capture more CO₂. At 288 K and 298 K, 15 L and 11 L of CO₂ could be adsorbed by 1 mol of 3-Amino-1-propanol, separately. However, when the temperature reached 328 K, 3-Amino-1-propanol only captured 9.7 L of CO₂. The speculated reason for this is that the solubility of CO₂ was lower under the condition of higher temperatures and that 3-Amino-1-propanol would evaporate at higher temperatures as well. In this case, 3-Amino-1-propanol could not adsorb CO₂ efficiently then. Combining the results of the two parts, 288 K of 3-Amino-1-propanol was optimal, and it could adsorb about 15 L of CO₂.

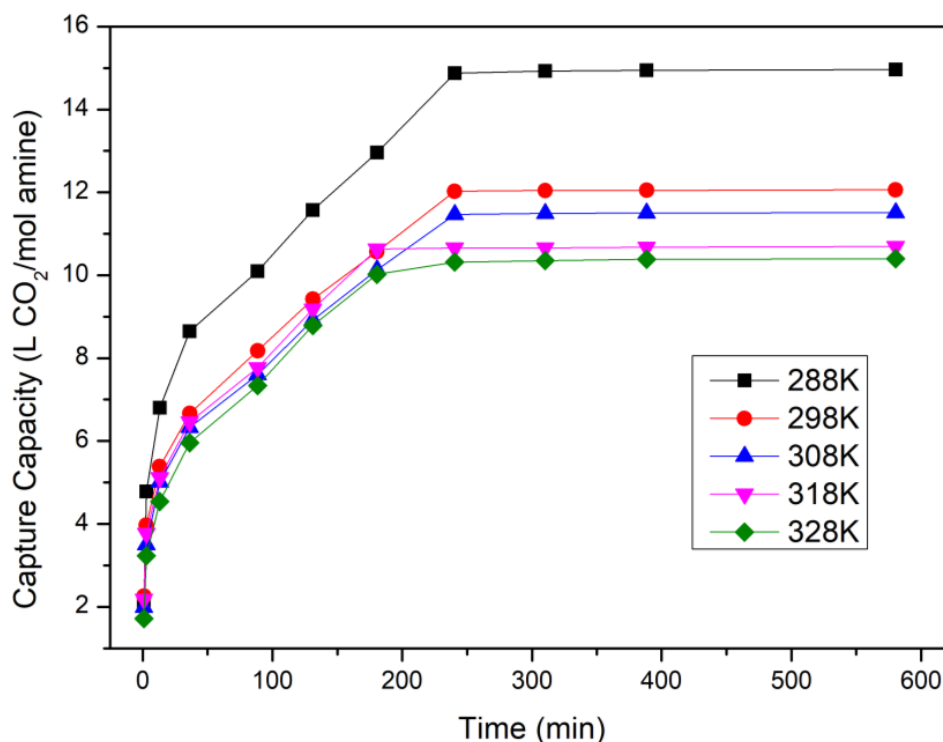


Figure 5. Saturated CO₂ capacity of 3-Amino-1-propanol at different temperatures.

3.4. XRD, SEM, and Whiteness Analyses of Magnesium Carbonate

After capturing CO₂ through 3-Amino-1-propanol at 288 K, moderate magnesium hydroxide from desalination brine was added into saturated 3-Amino-1-propanol. Magnesium hydroxide would then react with CO₂ and turn into magnesium bicarbonate solutions. Through heating the amine carriers, magnesium carbonate would be precipitated, and the amine carriers could be reused. The XRD pattern of magnesium carbonate is displayed in Figure 6, and the magnesium carbonate was in the form of nesquehonite. The molecular formula and crystal system of nesquehonite are MgCO₃·3H₂O and monoclinic [38–41]. To gain a deeper understanding of nesquehonite, the SEM analysis is revealed in Figure 7. The shape of nesquehonite was linear and acicular, and it coincided with the narrative in the other literature [41].

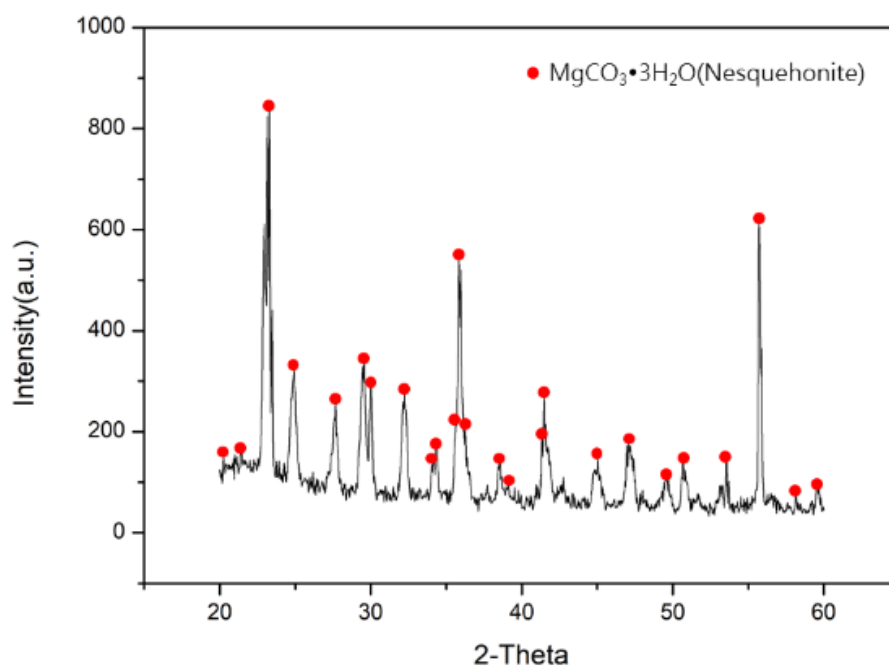


Figure 6. XRD analysis of magnesium carbonate.



Figure 7. SEM analysis of magnesium carbonate (nesquehonite).

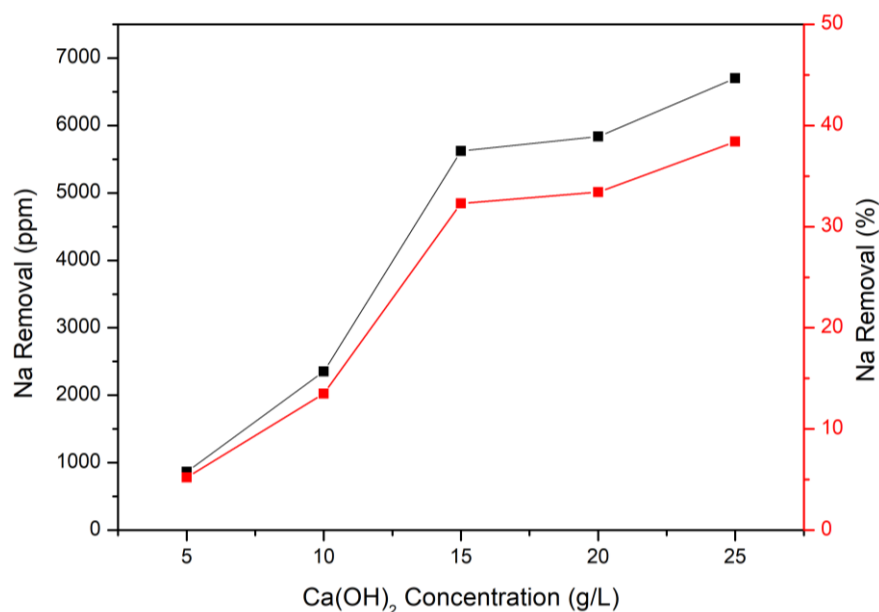
On the other hand, magnesium carbonate can be used as the coating material, and its index is whiteness. Whiteness is the degree of whiteness on the surface of a substance. If the whiteness is above 90, it can be the coating material or the paint ingredient. A comparison of the whiteness of commercial and experimental magnesium carbonate is shown in Table 3. To get a higher preciseness, three different samples of commercial and experimental magnesium carbonate were detected, and the average whiteness of commercial product and magnesium carbonate we obtained was 94.8 and 93.6, respectively. This means that the magnesium carbonate produced in this study has an applied value in other industries so as to reach resources' circulation.

Table 3. Whiteness of commercial product and experimental magnesium carbonate.

Magnesium Carbonate	Samples	Whiteness
Commercial product	Sample 1	94.9
	Sample 2	94.7
	Sample 3	94.8
Experimental magnesium carbonate	Sample 1	93.5
	Sample 2	93.5
	Sample 3	93.8

3.5. Modified Solvay Process-Removal of Sodium at Different $\text{Ca}(\text{OH})_2$ Concentrations

After finishing the amine carrier method, the modified Solvay process was implemented through calcium hydroxide and desalination brine. This process could not only adsorb CO_2 but also remove the sodium in the brine. The procedure was as follows: calcium hydroxide was added into pH 14 of brine and reacted as in Equation (2). The concentrations of $\text{Ca}(\text{OH})_2$ were set up from 5 g/L to 25 g/L, and the results are demonstrated in Figure 8. As Figure 8 illustrates, 5 g/L of $\text{Ca}(\text{OH})_2$ could only remove 1000 ppm of sodium, and the value would increase with the $\text{Ca}(\text{OH})_2$ concentration increasing. Under the condition of 25 g/L of $\text{Ca}(\text{OH})_2$, the sodium removal could reach about 7000 ppm, and the removal efficiency was 45%. The results seem to show that the concentration of $\text{Ca}(\text{OH})_2$ could increase continuously; however, excessive $\text{Ca}(\text{OH})_2$ would react with CO_2 first and produce calcium carbonate rather than sodium bicarbonate (It would interrupt the generation of sodium bicarbonate). Therefore, the optimal $\text{Ca}(\text{OH})_2$ concentration in this study was 25 g/L.

**Figure 8.** Removal of sodium at different $\text{Ca}(\text{OH})_2$ concentrations through modified Solvay process.

3.6. Modified Solvay Process-Removal of Sodium at Different Temperatures

The temperatures were set up from 288 K to 328 K in this study, and the fixed parameter was 25 g/L of calcium hydroxide. Figure 9 illustrates that an increase in the temperatures would decrease the removal efficiency of sodium. At 288 K, the sodium removal was about 7000 ppm, and it was only under 1000 ppm at 328 K. The main reasons were the solubilities of CO_2 and sodium bicarbonate. At higher temperatures, the solubility of CO_2 would decrease and make it challenging to conduct the reaction. On the other hand, even if the reaction progressed, the precipitated sodium bicarbonate was easily dissolved in the high-temperature aqueous solution [36] (The solubilities of sodium bicarbonate at

different temperatures are demonstrated in Table 4). Combining the above reasons, 25 g/L of $\text{Ca}(\text{OH})_2$ at 288 K was the optimal parameter for removing sodium. After removing sodium, the brine could then be released back into the ocean, or other valuable metals could be extracted in a further process. Sodium bicarbonate can be used in other industries as well in order to achieve the goal of a circular economy. In a nutshell, the modified Solvay process could adsorb 16 L of CO_2 per liter of brine with 25 g of $\text{Ca}(\text{OH})_2$ and reduce the side effect of sodium.

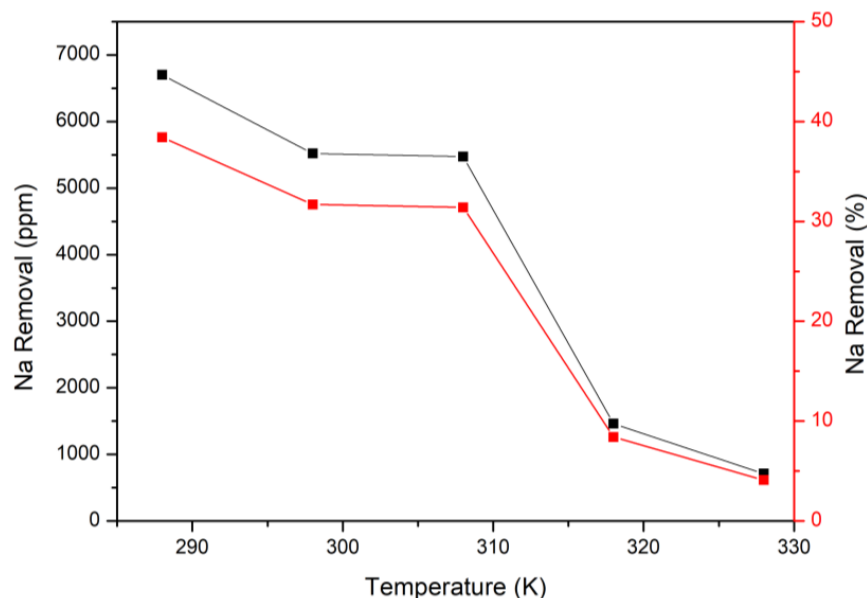


Figure 9. Removal of sodium at different temperatures through the modified Solvay process.

Table 4. Solubility of sodium bicarbonate at different temperatures.

Temperatures	288 K	298 K	308 K	318 K	328 K
Solubility (g/100 g water)	7.6	8.4	9.9	12.1	13.9

4. Conclusions

This study aims to recover magnesium and calcium to adsorb CO_2 and remove sodium through the amine carrier method and the modified Solvay process. The results reveal that the magnesium hydroxide and calcium hydroxide precipitation rates were 99.94% and 97.2%, separately. 288 K of 3-Amino-1-propanol could capture 15 L (26.9 g) of CO_2 first, and magnesium hydroxide could then react with 3-Amino-1-propanol in order to turn into magnesium carbonate. The XRD, SEM, and whiteness analyses of magnesium carbonate showed that it had an applied value in this study as well. Moreover, 25 g/L of $\text{Ca}(\text{OH})_2$ at 288 K was the optimal parameter for removing sodium and adsorbing CO_2 in the modified Solvay process. The efficiencies of sodium removal and capacity of CO_2 were 7000 ppm (45%) and 16 L (28.7 g), respectively. In sum, this research demonstrates a system that could capture CO_2 through amine carriers and brine. In addition, the high concentration of sodium in the brine was also decreased. This means that the study could reduce CO_2 emissions and the environmental problems caused by brine simultaneously.

Author Contributions: Conceptualization, C.-H.L. and P.-H.C.; methodology, C.-H.L. and W.-S.C.; validation, C.-H.L., P.-H.C. and W.-S.C.; formal analysis, C.-H.L.; investigation, C.-H.L.; data curation, C.-H.L. and P.-H.C.; writing—original draft preparation, C.-H.L.; writing—review and editing, C.-H.L.; visualization, C.-H.L.; supervision, W.-S.C. All authors have read and agreed to the published version of the manuscript.

Funding: This research received no external funding.

Acknowledgments: This work was supported by the Laboratory of Resource Circulation in the Dept. of Resources Engineering, National Cheng-Kung University.

Conflicts of Interest: The authors declare no conflict of interest.

References

1. Visser, P.M.; Verspagen, J.M.; Sandrini, G.; Stal, L.J.; Matthijs, H.C.; Davis, T.W.; Paerl, H.W.; Huisman, J. How rising CO₂ and global warming may stimulate harmful cyanobacterial blooms. *Harmful Algae* **2016**, *54*, 145–159. [[CrossRef](#)] [[PubMed](#)]
2. Lee, Z.H.; Sethupathi, S.; Lee, K.T.; Bhatia, S.; Mohamed, A.R. An overview on global warming in Southeast Asia: CO₂ emission status, efforts done, and barriers. *Renew. Sustain. Energy Rev.* **2013**, *28*, 71–81. [[CrossRef](#)]
3. Yoro, K.O.; Daramola, M.O. CO₂ emission sources, greenhouse gases, and the global warming effect. In *Advances in Carbon Capture*; Elsevier: Amsterdam, The Netherlands, 2020; pp. 3–28.
4. Rosa, L.P.; Ribeiro, S.K. The present, past, and future contributions to global warming of CO₂ emissions from fuels. *Clim. Chang.* **2001**, *48*, 289–307. [[CrossRef](#)]
5. Philander, S.G. *Encyclopedia of Global Warming and Climate Change: AE*; Sage: Thousand Oaks, CA, USA, 2008.
6. Mejía, A.; Nucete Hubner, M.; Ron Sánchez, E.; Doria, M. *The United Nations World Water Development Report-No 4-Water and Sustainability (A Review of Targets, Tools and Regional Cases)*; United Nations: San Francisco, CA, USA, 2012.
7. Wagnick, K. *IDA Worldwide Desalting Plants: Inventory Report No. 17*; Wagnick Consulting: Gnarrenburg, Germany, 2002.
8. Kim, I.; Yoo, Y.; Son, J.; Park, J.; Huh, I.-S.; Kang, D. Two-step mineral carbonation using seawater-based industrial wastewater: An eco-friendly carbon capture, utilization, and storage process. *J. Mater. Cycles Waste Manag.* **2020**, *22*, 333–347. [[CrossRef](#)]
9. Kang, D.; Lee, M.-G.; Jo, H.; Yoo, Y.; Lee, S.-Y.; Park, J. Carbon capture and utilization using industrial wastewater under ambient conditions. *Chem. Eng. J.* **2017**, *308*, 1073–1080. [[CrossRef](#)]
10. Al-Mamoori, A.; Krishnamurthy, A.; Rownaghi, A.A.; Rezaei, F. Carbon Capture and Utilization Update. *Energy Technol.* **2017**, *5*, 834–849. [[CrossRef](#)]
11. Stünkel, S.; Drescher, A.; Wind, J.; Brinkmann, T.; Repke, J.-U.; Wozny, G. Carbon dioxide capture for the oxidative coupling of methane process—A case study in mini-plant scale. *Chem. Eng. Res. Des.* **2011**, *89*, 1261–1270. [[CrossRef](#)]
12. Yeh, A.C.; Bai, H. Comparison of ammonia and monoethanolamine solvents to reduce CO₂ greenhouse gas emissions. *Sci. Total Environ.* **1999**, *228*, 121–133. [[CrossRef](#)]
13. Bai, H.; Yeh, A.C. Removal of CO₂ Greenhouse Gas by Ammonia Scrubbing. *Ind. Eng. Chem. Res.* **1997**, *36*, 2490–2493. [[CrossRef](#)]
14. Diao, Y.-F.; Zheng, X.-Y.; He, B.; Chen, C.-H.; Xu, X.-C. Experimental study on capturing CO₂ greenhouse gas by ammonia scrubbing. *Energy Convers. Manag.* **2004**, *45*, 2283–2296. [[CrossRef](#)]
15. Li, X.; Hagaman, E.; Tsouris, A.C.; Lee, J.W. Removal of Carbon Dioxide from Flue Gas by Ammonia Carbonation in the Gas Phase. *Energy Fuels* **2002**, *17*, 69–74. [[CrossRef](#)]
16. Pan, S.-Y.; Chang, E.; Chiang, P.-C. CO₂ Capture by Accelerated Carbonation of Alkaline Wastes: A Review on Its Principles and Applications. *Aerosol Air Qual. Res.* **2012**, *12*, 770–791. [[CrossRef](#)]
17. Li, Y.; Liu, C.; Sun, R.; Liu, H.; Wu, S.; Lu, C. Sequential SO₂/CO₂ capture of calcium-based solid waste from the paper industry in the calcium looping process. *Ind. Eng. Chem. Res.* **2012**, *51*, 16042–16048. [[CrossRef](#)]
18. Karimi, M.; de Tuesta, J.L.D.; Gonçalves, C.N.D.P.; Gomes, H.T.; Rodrigues, A.E.; Silva, J.A.C.; Mohsen, K.; José, A.S. Compost from Municipal Solid Wastes as a Source of Biochar for CO₂ Capture. *Chem. Eng. Technol.* **2020**, *43*, 1336–1349. [[CrossRef](#)]
19. Ibrahim, M.H.; El-Naas, M.H.; Zevenhoven, R.; Al-Sobhi, S.A. Enhanced CO₂ capture through reaction with steel-making dust in high salinity water. *Int. J. Greenh. Gas Control* **2019**, *91*, 102819. [[CrossRef](#)]
20. Olivares-Marín, M.; Maroto-Valer, M.M. Development of adsorbents for CO₂ capture from waste materials: A review. *Greenh. Gases Sci. Technol.* **2012**, *2*, 20–35. [[CrossRef](#)]
21. Kaithwas, A.; Prasad, M.; Kulshreshtha, A.; Verma, S. Industrial wastes derived solid adsorbents for CO₂ capture: A mini review. *Chem. Eng. Res. Des.* **2012**, *90*, 1632–1641. [[CrossRef](#)]
22. Pour, N.; Webley, P.; Cook, P.J. Potential for using municipal solid waste as a resource for bioenergy with carbon capture and storage (BECCS). *Int. J. Greenh. Gas Control* **2018**, *68*, 1–15. [[CrossRef](#)]
23. Ohenoja, K.; Rissanen, J.; Kinnunen, P.; Illikainen, M. Direct carbonation of peat-wood fly ash for carbon capture and utilization in construction application. *J. CO₂ Util.* **2020**, *40*, 101203. [[CrossRef](#)]
24. Dindi, A.; Quang, D.V.; Vega, L.F.; Nashef, E.; Abu-Zahra, M.R. Applications of fly ash for CO₂ capture, utilization, and storage. *J. CO₂ Util.* **2018**, *29*, 82–102. [[CrossRef](#)]
25. Mankar, J.S.; Rayalu, S.S.; Balasubramanian, R.; Krupadam, R.J. High performance CO₂ capture at elevated temperatures by using cenospheres prepared from solid waste, fly ash. *Chemosphere* **2021**, *284*, 131405. [[CrossRef](#)]
26. Sreenivasulu, B.; Sreedhar, I.; Reddy, B.M.; Raghavan, K.V. Stability and Carbon Capture Enhancement by Coal-Fly-Ash-Doped Sorbents at a High Temperature. *Energy Fuels* **2017**, *31*, 785–794. [[CrossRef](#)]
27. Skocek, J.; Zajac, M.; Ben Haha, M. Carbon Capture and Utilization by mineralization of cement pastes derived from recycled concrete. *Sci. Rep.* **2020**, *10*, 1–12.
28. Lu, L.; Guest, J.S.; Peters, C.A.; Zhu, X.; Rau, G.H.; Ren, Z.J. Wastewater treatment for carbon capture and utilization. *Nat. Sustain.* **2018**, *1*, 750–758. [[CrossRef](#)]

29. Dong, C.; Huang, G.; Cheng, G.; An, C.; Yao, Y.; Chen, X.; Chen, J. Wastewater treatment in amine-based carbon capture. *Chemosphere* **2019**, *222*, 742–756. [[CrossRef](#)] [[PubMed](#)]
30. Mustafa, J.; Aya, A.-H.M.; Al-Marzouqi, A.H.; El-Naas, M.H. Simultaneous treatment of reject brine and capture of carbon dioxide: A comprehensive review. *Desalination* **2020**, *483*, 114386. [[CrossRef](#)]
31. Galvez-Martos, J.-L.; Elhoweris, A.; Morrison, J.; Al-Horr, Y. Conceptual design of a CO₂ capture and utilisation process based on calcium and magnesium rich brines. *J. CO₂ Util.* **2018**, *27*, 161–169. [[CrossRef](#)]
32. El-Naas, M.H.; Al-Marzouqi, A.H.; Chaalal, O. A combined approach for the management of desalination reject brine and capture of CO₂. *Desalination* **2010**, *251*, 70–74. [[CrossRef](#)]
33. Kang, D.; Jo, H.; Lee, M.-G.; Park, J. Carbon dioxide utilization using a pretreated brine solution at normal temperature and pressure. *Chem. Eng. J.* **2016**, *284*, 1270–1278. [[CrossRef](#)]
34. Yoo, Y.; Kang, D.; Park, S.; Park, J. Carbon utilization based on post-treatment of desalinated reject brine and effect of structural properties of amines for CaCO₃ polymorphs control. *Desalination* **2020**, *479*, 114325. [[CrossRef](#)]
35. Dindi, A.; Quang, D.V.; Abu Zahra, M. Simultaneous carbon dioxide capture and utilization using thermal desalination reject brine. *Appl. Energy* **2015**, *154*, 298–308. [[CrossRef](#)]
36. El-Naas, M.H.; Mohammad, A.F.; Suleiman, M.I.; Al Musharfy, M.; Al-Marzouqi, A.H. A new process for the capture of CO₂ and reduction of water salinity. *Desalination* **2017**, *411*, 69–75. [[CrossRef](#)]
37. Carson, P.A. *Hazardous Chemicals Handbook*; Elsevier: Amsterdam, The Netherlands, 2002.
38. Montes-Hernandez, G.; Bah, M.; Renard, F. Mechanism of formation of engineered magnesite: A useful mineral to mitigate CO₂ industrial emissions. *J. CO₂ Util.* **2019**, *35*, 272–276. [[CrossRef](#)]
39. Unluer, C.; Al-Tabbaa, A. Green construction with carbonating reactive magnesia porous blocks: Effect of cement and water contents. In Proceedings of the International Conference on Future Concrete, Dubai, United Arab Emirates, 12–14 December 2011.
40. Yan, P.K.; Wang, B.; Gao, Y.J. Study on Synthesis of the High Aspect Ratios Nesquehonite Whiskers. *Adv. Mater. Res.* **2011**, *239*, 1118–1122. [[CrossRef](#)]
41. Stephan, G.; MacGillavry, C.H. The crystal structure of nesquehonite, MgCO₃ · 3H₂O. *Acta Crystallogr. Sect. B* **1972**, *28*, 1031–1033. [[CrossRef](#)]